

# Influence of Water Allocation and Freshwater Inflow on Oyster Production: A Hydrodynamic–Oyster Population Model for Galveston Bay, Texas, USA

## ERIC N. POWELL\*

Haskin Shellfish Research Laboratory  
Rutgers University  
6959 Miller Ave.  
Port Norris, New Jersey 08349, USA

## JOHN M. KLINCK

## EILEEN E. HOFMANN

Center for Coastal Physical Oceanography  
Crittenton Hall  
Old Dominion University  
Norfolk, Virginia 23529, USA

## MARGARET A. McMANUS

Ocean Sciences Department  
University of California Santa Cruz  
1156 High St.  
Santa Cruz, California 95064, USA

**ABSTRACT** / A hydrodynamic–oyster population model was developed to assess the effect of changes in freshwater inflow on oyster populations in Galveston Bay, Texas, USA. The population model includes the effects of environmental conditions, predators, and the oyster parasite, *Perkinsus marinus*, on oyster populations. The hydrodynamic model includes the effects of wind stress, river runoff, tides, and oceanic exchange on the circulation of the bay. Simulations were run for low, mean, and high freshwater inflow conditions under the present (1993) hydrology and predicted hydrologies for 2024

and 2049 that include both changes in total freshwater inflow and diversions of freshwater from one primary drainage basin to another.

Freshwater diversion to supply the Houston metropolitan area is predicted to negatively impact oyster production in Galveston Bay. Fecundity and larval survivorship both decline. Mortality from *Perkinsus marinus* increases, but to a lesser extent. A larger negative impact in 2049 relative to 2024 originates from the larger drop in fecundity under that hydrology. Changes in recruitment and mortality, resulting in lowered oyster abundance, occur because the bay volume available for mixing freshwater input from the San Jacinto and Buffalo Bayou drainage basins that drain metropolitan Houston is small in comparison to the volume of Trinity Bay that presently receives the bulk of the bay's freshwater inflow. A smaller volume for mixing results in salinities that decline more rapidly and to a greater extent under conditions of high freshwater discharge.

Thus, the decline in oyster abundance results from a disequilibrium between geography and salinity brought about by freshwater diversion. Although the bay hydrology shifts, available hard substrate does not. The simulations stress the fact that it is not just the well-appreciated reduction in freshwater inflow that can result in decreased oyster production. Changing the location of freshwater inflow can also significantly impact the bay environment, even if the total amount of freshwater inflow does not change.

The Galveston Bay estuarine system is located about 50 km south of Houston, Texas, USA. The bay is connected to the Gulf of Mexico by three passes, the primary one being Bolivar Roads, and receives most of its freshwater input from two rivers, the San Jacinto and the Trinity, with the primary water source being the Trinity River (Fisher and others 1972, Ward 1980, Arm-

strong 1982) (Figure 1). Along the main north–south axis of the bay is the Houston Ship Channel, which connects the Port of Houston with the Gulf of Mexico. On average, Galveston Bay is 2–3 m deep, with the exception of the Houston Ship Channel, which is presently 12.2 m deep.

Galveston Bay accounts for a significant fraction of the US production of the Eastern oyster, *Crassostrea virginica* (Quast and others 1988). Most of the oyster reefs are 1–3 m deep, but some are intertidal and, along the Houston Ship Channel, the reefs are up to 6 m deep (Powell and others 1995a). The most productive

**KEY WORDS:** Oyster; Estuary; Channelization; Salinity; Freshwater inflow; Larval survivorship; Fecundity; *Perkinsus marinus*

\*Author to whom correspondence should be addressed.

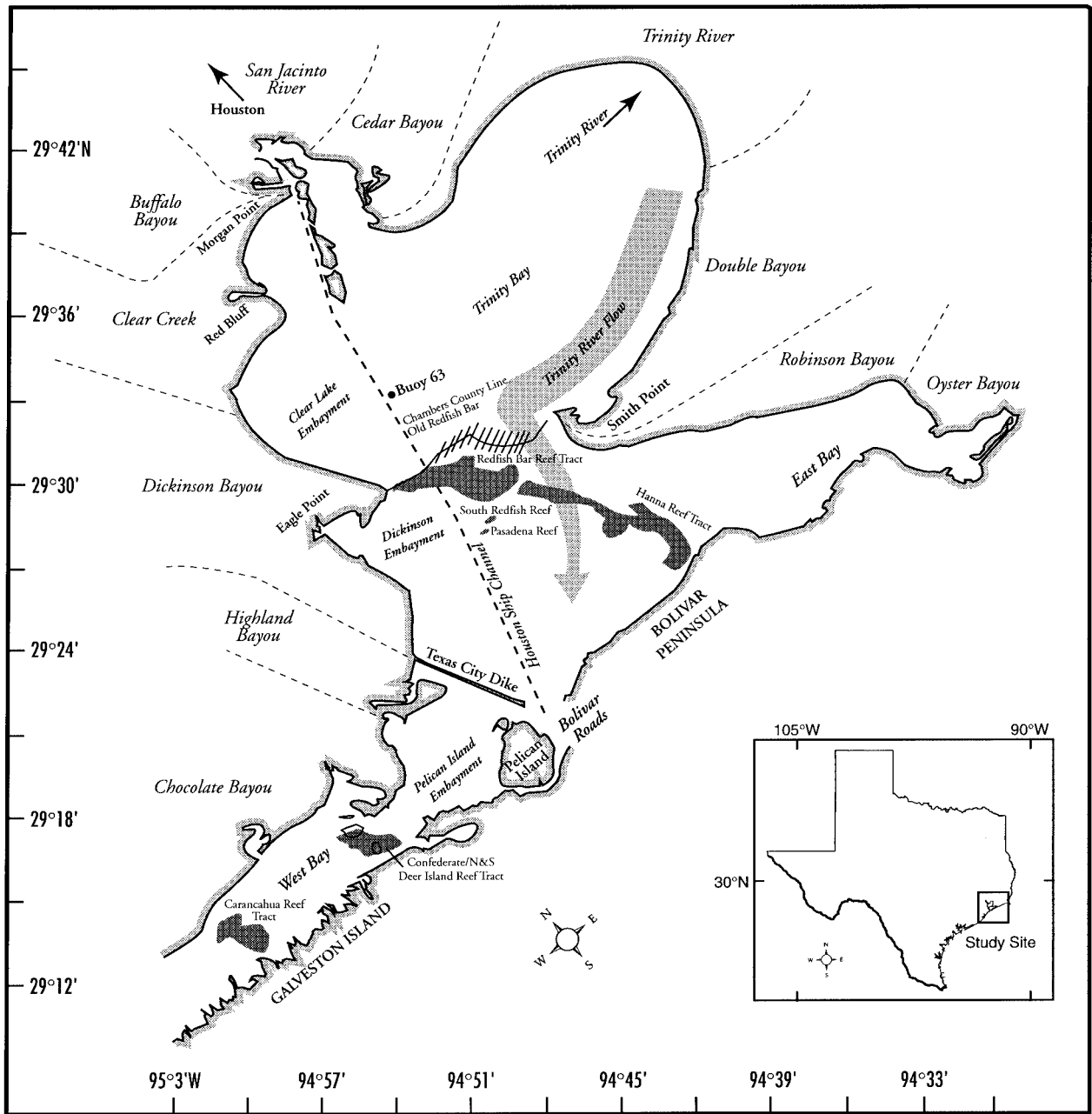


Figure 1. Map of Galveston Bay showing the locations of geographic features referred to in the text.

areas are adjacent to the ship channel and along the Redfish Bar reef tract that is bisected by the ship channel (Figure 1).

As population growth continues in coastal Texas, more pressure is put on limited freshwater resources. The Houston metropolitan area is a high population-growth area and, so, the allocation of freshwater is an issue. Water plans for the next 50 years address the issue of insufficient water in the San Jacinto watershed

to satisfy demand. In the near term, the implications for oyster production in Galveston Bay are twofold. First, freshwater inflow is likely to be reduced, particularly in the Trinity River drainage basin as Trinity River water is diverted to the Houston metropolitan area and to other metropolitan areas upstream (including Dallas). Second, the proportion of total freshwater inflow derived from the Trinity River watershed is likely to change as water is diverted to the metropolitan area of Houston

and is returned into the San Jacinto River and Buffalo Bayou drainage basins rather than the Trinity (Figure 1).

Farther into the future, plans call for the diversion of water from eastern Texas (e.g., the Sabine River) to the Houston metropolitan area. The implications for oyster production in Galveston Bay are again twofold. First, the total amount of freshwater inflow would increase. Second, this increase would, in the main, enter Galveston Bay through the San Jacinto River and Buffalo Bayou rather than the Trinity River.

Oysters are sensitive to changes in salinity. These changes in freshwater inflow may alter the bay's salinity structure and, as a consequence, impact the oyster populations. Salinity controls oyster predators and, most importantly, oyster diseases (Andrews and Ray 1988, Soniat and Brody 1988, Soniat and Gauthier 1989), with increases in salinity normally being associated with increased rates of mortality. Salinity also significantly influences oyster larval growth and survival (Davis 1958, 1964, Hidu and Haskin 1978) and physiological energetics (Butler 1949, Loosanoff 1953, Shumway 1982).

If a rule of thumb exists for oysters and freshwater inflow, it is that a reduction in freshwater inflow or an increase in saltwater intrusion will result in a reduction in oyster production because increased salinity increases the rate of oyster mortality from predation and disease. However, Powell and others (1995a) observed reef accretion down-estuary of the 15‰ isohaline in Galveston Bay, and Klinck and others (2002) concluded that additional saltwater intrusion from the proposed enlargement of the Houston Ship Channel would increase oyster production rather than decrease it. The implication is that reduced freshwater inflow or increased saltwater intrusion is not always deleterious. One aspect of this issue is that the location of saltwater and freshwater additions into the estuary may significantly alter oyster production by generating or eliminating disequilibria between the location of the hard substrate needed for oyster settlement and the necessary environmental conditions needed for growth and reproduction. Such disequilibria explain the results of Powell and others (1995a) and Klinck and others (2002) referred to earlier. To further investigate the relative importance of net additions of freshwater or saltwater and the effect of changes in the location of freshwater inflow on bay oyster production, a simulation model of oyster population dynamics was applied to the case of Galveston Bay. Simulations were designed to ascertain the likely influence of anticipated variations in freshwater inflow over the next 50 years on the bay's oyster populations.

## Modeled System—Galveston Bay

Figure 1 gives a synopsis of the names and locations of the topographic and other features of Galveston Bay referred to in this report. Powell and others (1995a) show the distribution of oyster reefs in Galveston Bay (their Figures 4–7) and review the history of the Galveston Bay reef system. Reef and unconsolidated shelly sediments comprise a total of 10,794.5 ha in Galveston Bay, most of which is distributed across the central bay (Redfish Bar-Hanna Reef tracts), along the Houston Ship Channel, and in the East and West Bay arms of Galveston Bay. Most is natural reef; however, about 18% of the total reef area is manmade, principally through the growth of reef on the dredge spoil shoulders of dredged channels. Galveston Bay is in a reef accretionary stage in most of its reaches, with considerable new reef developed in the central bay and along the Houston Ship Channel over the last 20 years (Powell and others, 1995a). Powell and others (1995a) determined that estuarine hydrodynamics and the salinity gradient are not now in equilibrium with the reef tracts. The disequilibrium between geology and physicochemical environment that has permitted the development of the present-day oyster industry in the bay [compare Galtsoff (1931) and Hofstetter (1990)], originates from barrier reef removal and channelization that have occurred principally since 1940. This disequilibrium is the primary reason for the rapid expansion of reef into unoccupied territory.

The principal sources of freshwater inflow are the San Jacinto River and Buffalo Bayou to the west and northwest and the Trinity River to the northeast (Figure 1). The Trinity River contributes most of the freshwater volume to the bay. The San Jacinto River and Buffalo Bayou waters flow primarily down the western shore of Galveston Bay between the shoreline and the Houston Ship Channel. Trinity River water exits the bay primarily by flowing down the eastern shore of Trinity Bay and then south around Smith Point and across Redfish Bar. Salt moves up-bay principally via the Houston Ship Channel and into the central deeper portion of Trinity Bay. The Houston Ship Channel effectively acts as a barrier to flow separating the much smaller San Jacinto/Buffalo Bayou-impacted western shore from the much larger eastern area that receives the bulk of the Trinity River flow. Both East and West Bay arms are less hydrodynamically active. Flow into West Bay is minimized by the Texas City Dike, and flow into East Bay is minimized by the bypassing of Trinity River water as it flows south of Smith Point to Bolivar Roads (the primary inlet to the Gulf of Mexico) (Figure 1). Sections of the bay, then, operate quasiindependently

with respect to the hydrodynamic and salinity regime, and this results in significant spatial differences in oyster production even within the same salinity zone.

The Houston Ship Channel is one of the narrowest ship channels in the country. A program is in place now to enlarge the Houston Ship Channel from 122 m across and 12.2 m deep to 161.5 m across and 13.7 m deep, increasing the cross-sectional area by a factor of 1.49. As most of the saltwater entering this bay enters through this channel, the significantly larger cross-sectional area would suggest a significantly larger volume transport of salt into Galveston Bay as a result of channel enlargement. Klinck and others (2002) evaluated the influence of channel enlargement on oyster production. Oyster abundance and biomass were predicted to increase moderately after channel enlargement. Declines in oyster biomass were noted in most simulations in down-bay reaches. These declines were more than balanced by increased abundance and biomass up-bay. This distribution of effect was explained by two primary consequences of channel enlargement, an increase in mortality from *Perkinsus marinus* down-bay and an expansion of the salinity gradient up-bay. Inasmuch as channelization is anticipated to significantly affect the bay environment over the next 50 years, we evaluated the impact of changes in bay hydrology using the present ship channel configuration and the larger configuration that will probably be in place by 2024.

## The Hydrodynamic–Oyster Population Model

### The Oyster Model

Three models were combined to simulate the effects of environmental variability on the population structure of the Eastern oyster. The first model, a time-dependent postsettlement population-dynamics model, simulates the growth, reproduction, and mortality of the benthic phase of the oysters' life history. Submodels associated with the postsettlement model include: a time-dependent submodel of the transmission and proliferation of the parasite, *Perkinsus marinus*; a predation submodel simulating the effects of crabs and drills; and a competition submodel simulating the competitive effect of other filter feeders on oyster food supply. The second model, a time-dependent larval model, simulates larval growth and mortality during the planktonic larval phase. The final model is a three-dimensional circulation model developed by the US Army Corps of Engineers for Galveston Bay (Berger and others 1995). The circulation model provides horizontal velocity and salinity distributions on a finite element grid that was used to represent the bay geometry. Element-averaged

flow and salinity, obtained from the circulation model, are input to the postsettlement model. The element-averaged salinity is input to the larval model.

The postsettlement model runs within each grid element that contains oyster reef and the larval model is operative in those grid elements where viable spawns occur. The postsettlement and larval models also use as inputs bay-wide measurements of monthly averaged food and total suspended solids (TSS) distributions and an hourly temperature time series. These models and the associated environmental data are described in Klinck and others (2002) and Deksheniaks and others (2000). A brief description of the models is presented here.

*Postsettlement population dynamics model.* The time-dependent postsettlement model simulates the benthic phase of the oyster life cycle. This model and its application are described in Powell and others (1992, 1997) and Hofmann and others (1992). The model is an energy flow model based on the simple relationship between net production,  $NP$ , somatic,  $Pg$ , and reproductive,  $Pr$ , tissue growth, assimilation,  $A$ , and respiration,  $R$ :

$$NP = Pg + Pr = A - R. \quad (1)$$

*Larval model.* The larval model is designed to simulate the development of oyster larvae through the planktonic period of the oysters' life history and is described by Deksheniaks and others (1993, 1997). Oyster larvae are roughly 65  $\mu\text{m}$  in diameter after fertilization and grow to a length of roughly 335  $\mu\text{m}$ , at which time they are competent to settle into the benthic oyster community. The change in larval number with time is determined by growth processes that themselves are determined by four primary environmental factors: temperature, salinity, food concentration, and TSS, and mortality processes that include failure for the egg to be fertilized, the effect of siltation on eggs and the earliest larval stages, inherent genetic variability of the larvae, predation, extremes in environmental factors, the inability to find adequate reef at the time of metamorphosis, and loss during metamorphosis.

*Perkinsus marinus disease.* Parasitism by *P. marinus* reduces oyster growth and fecundity. Additionally, under high levels of infection, oyster mortality occurs. In the oyster population model, the primary effects of *P. marinus* infection on oysters are a reduction in oyster filtration rate and disease-induced mortality (Hofmann and others 1995). The loss of energy to *P. marinus* is an additional loss from oyster net production, and is represented as:

$$NP = A - R - E \quad (2)$$

where  $E$  is the energy lost to *P. marinus*. The infection intensity of *P. marinus*, and hence the effect of *P. marinus* on the oyster, is modulated by temperature and salinity with cell proliferation usually occurring when temperatures exceed 20°C and salinities exceed 20‰.

*Predation submodel.* Two predators, the oyster drill (*Thais haemastoma*) and a generic crab [representative of the blue crab (*Callinectes sapidus*) and various mud crabs such as *Panopeus herbstii*], were included as external factors affecting oyster production. Details of this model are provided by Powell and others (1997). The predation models for crabs and drills were based on handling times obtained from laboratory measures of consumption rate under specified conditions. The daily consumption rates, modified by temperature, salinity, and prey density, were calculated for each oyster size class assuming that the differences in the predator's experimentally determined consumption rates among the prey size classes reflected the fraction of the time that these predators would spend feeding on each of these size classes, were they all present in equal abundance. Then, we reallocated time spent feeding so that an abundant size class of lower optimal yield might nevertheless be consumed more frequently because of its proportionally higher contribution to the prey population.

*Competition submodel.* Competition for food is believed to be important on oyster reefs. In Galveston Bay and elsewhere in the region (Moore 1907, Engle and Chapman 1953), *Brachidontes* mussels are the other dominant filter feeder on reefs. Mussel ingestion rate was parameterized by standard equations used for bivalves given in Powell and Stanton (1985) and Powell and others (1992).

#### The Hydrodynamic Model

A three-dimensional finite element circulation model was developed for Galveston Bay and the surrounding offshore region by the US Army Corps of Engineers (Berger and others 1995, McAdory and others 1995). The circulation model is three-dimensional with the exception of the West Bay region west of the Pelican Island Embayment and the offshore areas where the model is two dimensional. The element-averaged water velocities obtained from the circulation model are input to the postsettlement model, and the element-averaged salinities are input to the postsettlement and larval models.

The finite element model provides simulations of the horizontal and vertical circulation and salinity distributions in Galveston Bay obtained from the momen-

tum equations, the volume continuity equation, and the advection–diffusion equation for salinity transport. The momentum equations are of the form:

$$\frac{\delta u}{\delta t} + \nabla \cdot (\vec{v}u) - fv = -\frac{1}{\rho} \frac{\delta P}{\delta x} + \nabla \cdot (A_H \nabla u) \quad (3)$$

$$\frac{\delta v}{\delta t} + \nabla \cdot (\vec{v}v) + fu = -\frac{1}{\rho} \frac{\delta P}{\delta y} + \nabla \cdot (A_H \nabla v) \quad (4)$$

$$\frac{\delta w}{\delta t} + \nabla \cdot (\vec{v}w) = -\frac{1}{\rho} \frac{\delta P}{\delta z} + \nabla \cdot (A_V \nabla w) - g \quad (5)$$

where  $u$ ,  $v$ , and  $w$  are the east–west ( $x$ ), north–south ( $y$ ) and vertical ( $z$ ) components of the time-varying ( $t$ ) velocity, respectively. The last term on the left side of equations 3 and 4 represents the Coriolis effect, where  $f$  is the Coriolis parameter. The terms on the left side of equations 3–5 represent changes due to pressure and to horizontal and vertical diffusion, where the values of the diffusion coefficients ( $A_H$  and  $A_V$ ) differ in the horizontal and vertical directions. The final term in equation 5 represents the effects of gravity.

The equation for continuity of volume is written as:

$$\frac{\delta u}{\delta x} + \frac{\delta v}{\delta y} + \frac{\delta w}{\delta z} = 0 \quad (6)$$

and that for advection and diffusion of salinity ( $S$ ) is written as

$$\frac{\delta S}{\delta t} + \nabla \cdot (\vec{v}S) - \nabla \cdot (\vec{K} \nabla S) = \theta_s \quad (7)$$

where  $S$  is expressed in parts per thousand and  $\theta_s$  is a source or sink of salinity.

#### Model Implementation and Environmental Forcing

*Freshwater inflow.* Freshwater inflow data for Galveston Bay were obtained from the US Geological Survey and the Texas Water Development Board for the period 1941–1987. Total freshwater inflow was calculated for each year and the years divided into the top 20% inflow years, the bottom 20% inflow years, and the middle 60% inflow years (Figure 2A). Monthly averages were then calculated for these three data sets which yielded freshwater inflow time series characteristic of high, low and mean freshwater inflow years, respectively (Fig. 2A). In a typical year, freshwater inflow is high in the spring and low in the late summer and fall. High freshwater inflow years are characterized by higher inflows in all months, but most of the increased inflow occurs in the spring months. Low inflow years are characterized by lower inflows in all months, but most of the inflow reduction occurs due to the reduction of inflow during the spring. The three time series for freshwater inflow were used in the hydrodynamic model

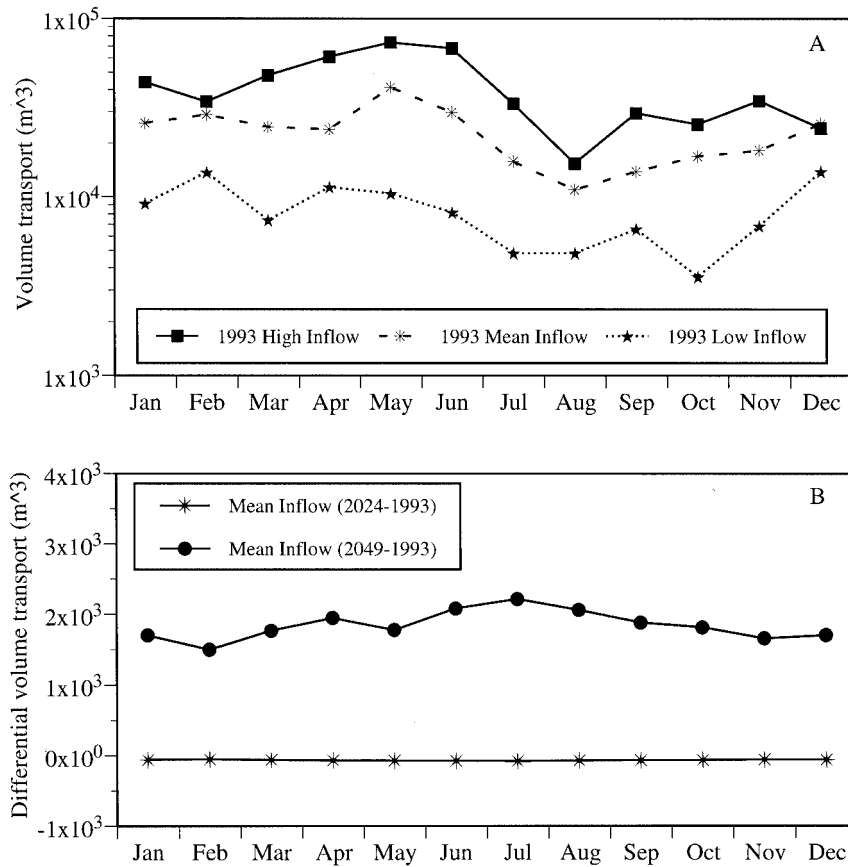


**Figure 2.** (A) Plot of total freshwater inflow into Galveston Bay during average high, mean, and low inflow years, under present (1993) conditions of water usage. (B) Monthly changes in total freshwater inflow anticipated for 2024 and 2049 relative to 1993. Anticipated volume changes are based on upstream additions and deletions and so are independent of total freshwater inflow rates under high, mean and low inflow conditions. Hence, only one case is given.

to obtain time series of salinity and water velocity for each freshwater inflow condition.

The influence of three hydrologies was investigated: the present (1993) hydrology and hydrologies anticipated for 2024 and 2049. The anticipated future hydrologies were obtained from the Texas Water Plan and the Houston Water Master Plan as they existed in the first half of the decade of the 1990s. Three separate processes are expected to influence freshwater inflow over the first half of the 21st century. These are: (1) the permanent removal of water from upstream watersheds, (2) the diversion of water from one drainage basin to another, and (3) the diversion of water from other watersheds into the Galveston Bay watershed. Each of these results from the need to fulfill the freshwater needs of the Houston metropolitan area that is located, in large measure, in the San Jacinto River and Buffalo Bayou watersheds draining into Galveston Bay (Figure 1).

The anticipated changes in total freshwater inflow

into Galveston Bay in 2024 and 2049 relative to the 1993 freshwater inflow are shown in Figure 2B. A slight drop in freshwater inflow is anticipated in 2024 due to upstream water diversions that are not returned into any Galveston Bay watershed. A substantial increase in freshwater inflow is anticipated in 2049 as water is diverted from remote watersheds (e.g., the Sabine River) to watersheds draining into Galveston Bay.

At least as important is the transfer of freshwater from one drainage basin to another within the Galveston Bay watershed. Much of the total freshwater inflow into Galveston Bay in 1993 came from the Trinity River (Figure 3A). Water transfers within the Galveston Bay system involve the removal of freshwater from the Trinity River drainage basin, thereby reducing freshwater inflow into Trinity Bay (Figure 3B,C). Inasmuch as freshwater supplies the needs of the Houston metropolitan area, the diverted water must ultimately come back into Galveston Bay, but via the San Jacinto River and Buffalo Bayou drainage basins rather than

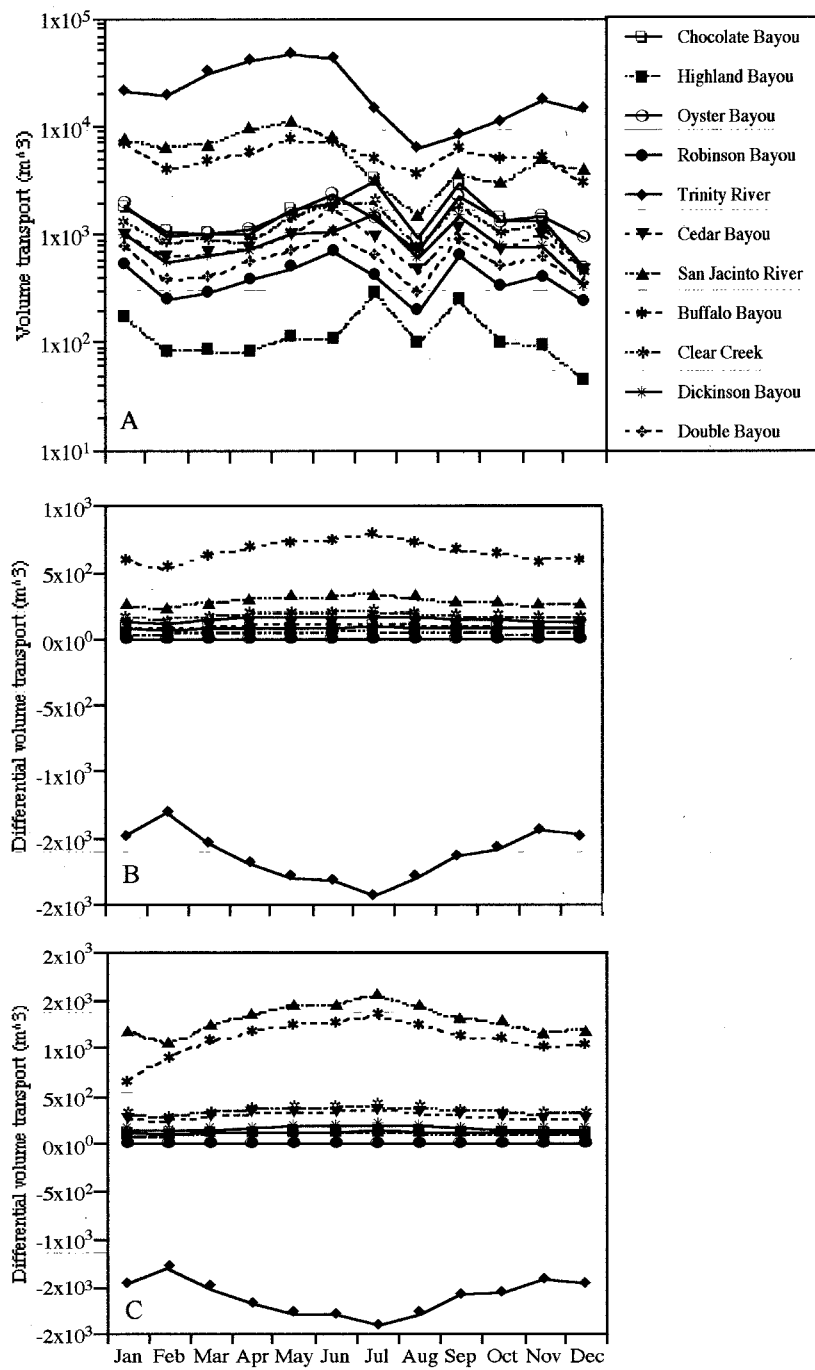


**Figure 3.** (A) Freshwater inflow by water drainage basin for each of the 11 drainage basins configured in the hydrodynamic model, under present-day average mean inflow conditions. (B) Difference in volume transport in each drainage basin between the anticipated situation in 2024 and the present-day (1993). (C) Difference in volume transport in each drainage basin between the anticipated situation in 2049 and the present-day.

the Trinity River drainage basin (US ACE 1995a). Thus, the 2024 hydrology contains a moderate decrease in freshwater inflow relative to 1993 and a significant redistribution of freshwater inflow into the estuary, and

this redistribution is significant under high, medium, and low freshwater inflow years. By 2030, all available San Jacinto and Trinity Basin water supplies are assumed to be used with almost all increases in water use

coming from transfers of water from nearby drainage basins. The 2049 hydrology retains the proportionately increased flows dictated by diversion of Trinity River water into the San Jacinto River and Buffalo Bayou drainage basins, but also includes higher freshwater inflows overall than in 2024 due to the transfer of water from watersheds beyond the Galveston Bay watershed into these same drainage basins (Figure 3C).

*Temperature.* Temperature values input to the oyster model were derived from hourly air temperature data for 1984 obtained from the Houston International Airport (NCDC 1985). Year 1984 was characterized by average temperatures in nearly every month and by near-mean freshwater inflow. These temperature values were applied uniformly across the Bay system.

*Predator distributions.* Time-invariant size frequencies and the spatial distribution of oyster drills, crabs, and mussels were obtained from the Galveston Bay National Estuary Program (GBNEP) health assessment (Song 1994) that occurred over a three-week period in April and May of 1992. During this time, 51 sites from all major reefs in the Galveston Bay system were intensively sampled. These 51 sites were used as a basis to calculate the size frequency and spatial distribution of oyster drills, crabs, and mussels in each grid element of the finite-element hydrodynamic model by assigning each sample site to a surface grid element and assigning the measured variable (e.g., crab abundance) to each of the corner nodes of this element. Distances ( $D_{i,j}$ ) were calculated from each defined node to all other nodes. The value of each unknown node ( $U_j$ ) was obtained as the distance-corrected mean of the known nodes ( $K_i$ ) where

$$U_j = \sum_i^n \frac{D_{i,j}^{-2}}{\sum_{l=1}^n D_{l,j}^{-2}} K_i \quad (8)$$

The variable value for each unsampled surface grid element was then obtained as the mean of the corner nodes.

*Food distribution.* Chlorophyll *a* and TSS were sampled (surface and near-bottom) at 32 sites at monthly intervals between October 1991 and September 1992 (Powell and others 1995b). Element values were obtained using equation (8) and, for chlorophyll, converted to food (milligrams AFDW per liter) using the total lipid, carbohydrate, and protein conversion of Soniat and others (1998). The TSS and food concentrations supplied to oysters in the oyster-circulation model come from the near-bottom samples. The food and TSS concentrations supplied to larvae are the averages of surface and near-bottom observations. Areas

of high food availability for oysters, averaging 2.2 mg AFDW/liter, are located to the east of the Houston Ship Channel. The areas of low food availability to oysters, averaging 1.6 mg AFDW/liter, are located within or to the west of the Houston Ship Channel (Dekshenieks and others 2000). With the exception of the Pelican Island Embayment, areas of high TSS, averaging 0.14 g/liter, fall to the east of the ship channel. Areas of low TSS, averaging 0.07 g/liter, are in the northern reaches of, or to the west of, the Houston Ship Channel (Dekshenieks and others 2000). TSS in Galveston Bay consists primarily of suspended sediment and refractive detrital material (Wilson-Ormond and others 1997). Consequently, TSS acted principally to reduce oyster filtration rates as a consequence of higher sediment loads, rather than to increase oyster food supply. The same food supply and TSS time series were used for all simulations because numerical models were not available. Consequently, the influence of changes in bay hydrodynamics and freshwater inflow on these variables has not been assessed.

*Numerical integration.* The coupled postsettlement/larval model was solved numerically using an implicit (Crank-Nicholson) time stepping scheme. Each model simulation was run for 2 years with a time step of 1 hour. Data for year 2 are used for interpretation. Data for year 1 are not used for interpretation because *Perkinsus marinus* prevalence and infection intensity had not yet equilibrated with environmental conditions. Furthermore, the initial abundance and size frequency of oysters used, which was the same for each element of the bay to make comparisons more easily interpreted, contained individuals too large to be supported by the food supply present in a number of bay sections. This is one reason that oysters are smaller on some reefs than on others. The size-frequency distribution comes into equilibrium with the available food supply by the end of year one.

## Data Presentation

Fifteen simulations were run for this analysis. These were Galveston Bay under the present (1993) configuration of the Houston Ship Channel and the present (1993) hydrology, during a year characterized by (1) high, (2) mean, and (3) low freshwater inflow (cf. Figure 2), simulations of the same three freshwater inflow scenarios, but using the 2024 hydrology (4–6) (cf. Figure 3B), simulations of the same three freshwater inflow scenarios, but using the 2049 hydrology (7–9) (cf. Figure 3C), and simulations of the same three hydrologies for 2024 and 2049, but with the Houston Ship Channel enlarged to 161.5 m across and 13.7 m deep (10–15).

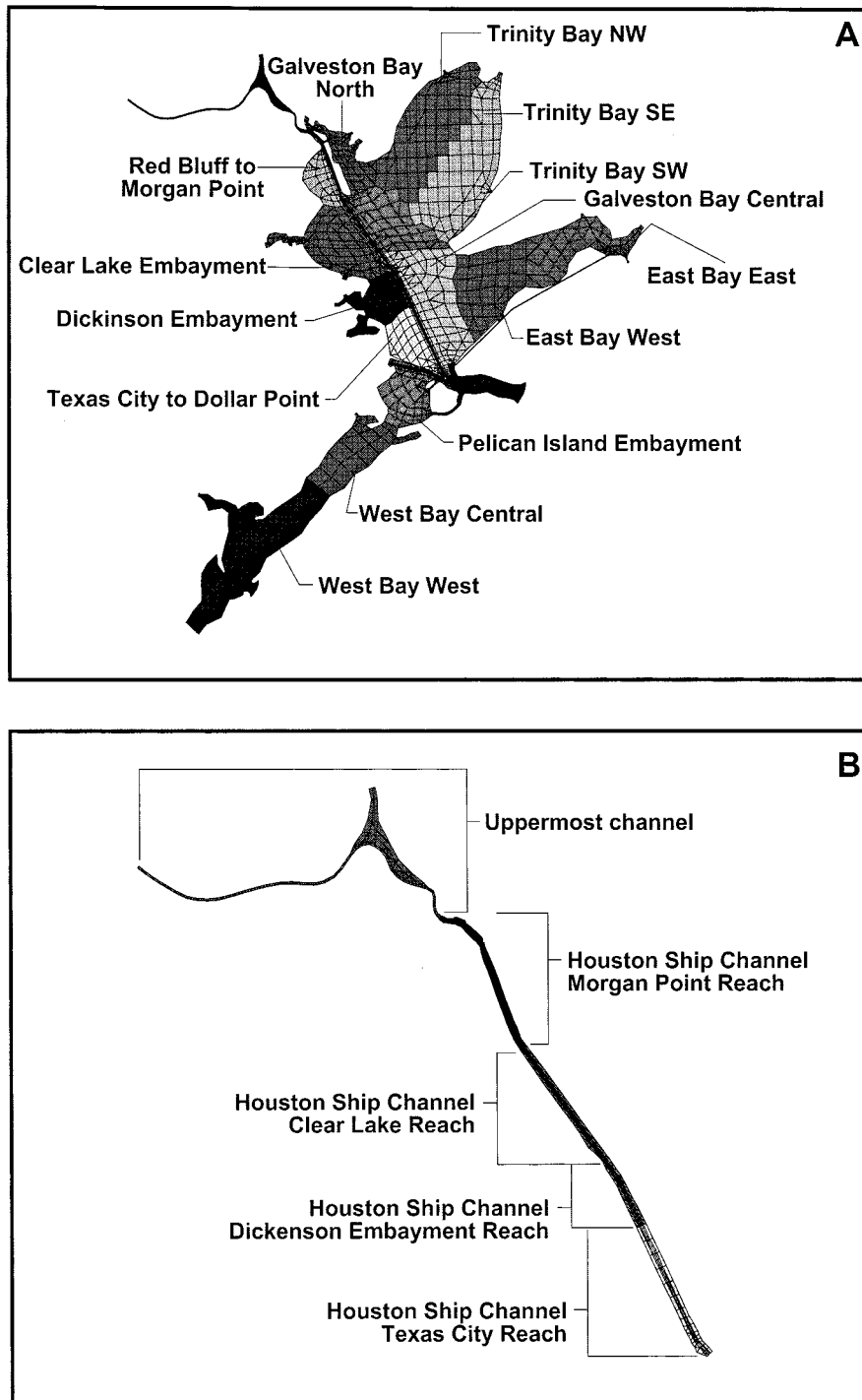


**Figure 4.** The 18 bay sections used for calculation of channel impacts.

Results were tabulated for the entire bay system and for 18 bay subdivisions delineated by observed differences in food supply, TSS level, and salinity (Figure 4). Although the model provides estimates of many oyster population characteristics, this analysis focuses on

total abundance, the abundance of market-size ( $\geq 76$  mm) oysters, fecundity, larval survivorship, and the influence of *P. marinus* disease and low salinity on oyster mortality.

Low and high freshwater inflows for each hydrology

(present, 2024, 2049) were computed using the lowest 20% of the yearly freshwater inflows and the highest 20% over a 46-year period. Consequently, average results for each hydrology were calculated as the weighted averages of the values obtained for the low, mean, and high freshwater inflow scenarios for that hydrology in accordance with this apportionment scheme:

$$\begin{aligned} \text{average for hydrology} = & \\ & 0.2 * \text{low inflow value} + \\ & 0.6 * \text{mean inflow value} + \\ & 0.2 * \text{high inflow value.} \quad (9) \end{aligned}$$

The effect of the wider and deeper ship channel summed over a 50-year assessment time span (1999–2049) was obtained by weighting the hydrologies according to their position in the 50-year time line and calculating a weighted mean value. The present hydrology was allocated 25% of the 50-year time span, the 2024 hydrology 50% of the 50-year time span, and the 2049 hydrology 25% of the 50-year time span:

$$\begin{aligned} \text{average for hydrology} = & \\ & 0.25 * 1993 \text{ hydrology value} + \\ & 0.50 * 2024 \text{ hydrology value} + \\ & 0.25 * 2049 \text{ hydrology value} \quad (10) \end{aligned}$$

#### Verification

The hydrodynamics model was extensively verified using data obtained from a series of moorings deployed throughout the Galveston Bay system (Berger and others 1995). The oyster population dynamics model was examined by a peer-review committee that extensively evaluated simulation accuracy (US ACE 1995b). Deksheniaks and others (2000) present base case simulations for the three freshwater inflow scenarios, 1993 hydrology, and original channel configuration. Deksheniaks and others (2000) also review the agreement of model simulation with field observation for the mean freshwater inflow case and observed good agreement overall. Only two bay regions require cautionary notes.

Simulated oyster densities in the Pelican Island Embayment frequently were high even though few oysters are present today in the area. This embayment is connected directly to the primary inlet, Bolivar Roads, and its connection with the main bay system is limited by the Texas City Dike (Figure 1). In all likelihood, a high flushing rate reduces recruitment in this embayment. The combined oyster–hydrodynamics model does not explicitly allow larval transport between finite element cells and, so, conditions in this embayment are not simulated adequately. It is interesting, however, that

the northern shore of this embayment, where the highest oyster production occurs in the simulations, at one time sustained the primary oyster fishery in Galveston Bay (Galtsoff 1931), a fishery that failed after the erection of the Texas City Dike.

The results for West Bay are also likely to be less robust than for the remainder of Galveston Bay. The finite element grid used in the hydrodynamics model for West Bay did not include the restriction in flow between North and South Deer Island nor did it contain the Intracoastal Waterway, which diverts freshwater inflow away from the central part of West Bay (Figure 1). Most of the West Bay hydrodynamics was simulated using a vertically averaged model (2-D), whereas most of the remainder of the bay circulation was simulated using the full 3-D model. Despite these short-comings, the simulated oyster populations followed the trends observed in West Bay. Production was normally highest near South Deer Island and lowest in the Carancahua Reef area. Nevertheless, these short-comings suggest that estimates for West Bay should be treated more cautiously than estimates for other areas. Because the acreage of reef in West Bay is relatively large, West Bay has a disproportionate contribution to Galveston Bay wide totals. Thus, Galveston Bay-wide totals should also be treated cautiously.

Finally, the high freshwater inflow simulation generated unusually low standing stocks in areas where low-salinity mortality was significant because larval survivorship was nil and transport of oyster larvae into these regions from the surrounding bay system was not allowed. Accordingly, standing stocks dropped below levels normally observed. However, the fact that local recruitment provided realistic estimates of standing stocks over wide areas of Galveston Bay and under a range of freshwater inflow conditions is noteworthy. It suggests that larval mixing is not as consequential in this bay as might normally be thought to be the case (Seliger and others 1982, Hill 1991, Deksheniaks and others 1996). The long water residence time (Armstrong 1982) and the fact that bay sections are clearly delineated by natural boundaries determined by bay geography and hydrodynamics probably explain the success of the “local-source” assumption.

## Results

### Perspective

The results of the 15 simulations are presented in terms of comparisons between selected hydrologies. This permits a direct evaluation of the effect of changes in the environment on the oyster populations. The comparisons are based on the fraction of total reef area

Table 1. Fraction of total bay acreage of oyster reef in Galveston Bay in which market-size or total oyster abundance increased with the 2024 or 2049 hydrology compared to the 1993 hydrology under conditions of low, mean, and high freshwater inflow and the present or the enlarged ship channel configuration<sup>a</sup>

| Location  | High inflow     |                  | Mean inflow     |                  | Low inflow      |                  | Time-weighted inflow |                  |
|---|-----------------|------------------|-----------------|------------------|-----------------|------------------|----------------------|------------------|
|   | Total abundance | Market abundance | Total abundance | Market abundance | Total abundance | Market abundance | Total abundance      | Market abundance |
| 2024 vs 1993 hydrology, present channel configuration |                 |                  |                 |                  |                 |                  |                      |                  |
| West Bay  | 0.044           | 0.358            | 0.014           | 0.040            | 0.000           | 0.129            | 0.017                | 0.121            |
| Trinity Bay   | 0.204           | <u>0.566</u>     | <u>0.710</u>    | <u>0.507</u>     | 0.273           | <u>0.668</u>     | <u>0.522</u>         | <u>0.551</u>     |
| Galveston Bay, North                                  | 0.074           | <u>0.580</u>     | 0.083           | 0.478            | <u>0.675</u>    | <u>0.563</u>     | 0.199                | <u>0.516</u>     |
| East Bay  | 0.277           | 0.458            | <u>0.529</u>    | <u>0.657</u>     | <u>0.578</u>    | 0.213            | 0.488                | <u>0.529</u>     |
| Galveston Bay, South                                  | 0.368           | <u>0.546</u>     | 0.290           | 0.356            | <u>0.520</u>    | <u>0.513</u>     | 0.352                | 0.425            |
| Bay totals  | 0.203           | 0.482            | 0.222           | 0.327            | 0.385           | 0.368            | 0.251                | 0.367            |
| 2049 vs 1993 hydrology, present channel configuration |                 |                  |                 |                  |                 |                  |                      |                  |
| West Bay  | <u>1.000</u>    | 0.059            | 0.014           | 0.040            | <u>0.531</u>    | 0.236            | 0.315                | 0.083            |
| Trinity Bay   | 0.258           | 0.279            | 0.000           | 0.143            | 0.188           | <u>0.726</u>     | 0.089                | 0.287            |
| Galveston Bay, North                                  | 0.011           | 0.318            | 0.020           | 0.221            | 0.336           | 0.409            | 0.082                | 0.278            |
| East Bay  | 0.000           | 0.336            | <u>0.551</u>    | 0.395            | <u>0.527</u>    | <u>0.525</u>     | 0.436                | 0.409            |
| Galveston Bay, South                                  | 0.085           | 0.207            | 0.127           | 0.159            | <u>0.587</u>    | 0.451            | 0.211                | 0.227            |
| Bay totals  | 0.346           | 0.201            | 0.130           | 0.165            | <u>0.505</u>    | 0.400            | 0.248                | 0.219            |
| 2024 vs 1993 hydrology, enlarged ship channel         |                 |                  |                 |                  |                 |                  |                      |                  |
| West Bay  | 0.436           | 0.000            | 0.494           | 0.440            | 0.455           | 0.440            | 0.475                | 0.352            |
| Trinity Bay   | <u>0.824</u>    | <u>0.967</u>     | <u>0.536</u>    | <u>0.670</u>     | <u>0.534</u>    | <u>0.713</u>     | <u>0.593</u>         | <u>0.738</u>     |
| Galveston Bay, North                                  | <u>0.873</u>    | <u>0.877</u>     | <u>0.563</u>    | <u>0.717</u>     | 0.483           | <u>0.630</u>     | <u>0.609</u>         | <u>0.731</u>     |
| East Bay  | 0.007           | 0.482            | 0.084           | 0.320            | 0.108           | 0.366            | 0.074                | 0.361            |
| Galveston Bay, South                                  | <u>0.533</u>    | <u>0.501</u>     | <u>0.559</u>    | <u>0.578</u>     | 0.364           | 0.485            | <u>0.515</u>         | <u>0.544</u>     |
| Bay totals  | 0.496           | 0.425            | 0.472           | <u>0.526</u>     | 0.381           | 0.487            | 0.459                | 0.498            |
| 2049 vs 1993 hydrology, enlarged ship channel         |                 |                  |                 |                  |                 |                  |                      |                  |
| West Bay  | 0.436           | 0.000            | 0.494           | 0.440            | 0.455           | 0.440            | 0.475                | 0.352            |
| Trinity Bay   | <u>0.771</u>    | <u>0.854</u>     | 0.462           | <u>0.641</u>     | <u>0.585</u>    | <u>0.680</u>     | <u>0.548</u>         | <u>0.692</u>     |
| Galveston Bay, North                                  | <u>0.812</u>    | <u>0.926</u>     | <u>0.541</u>    | <u>0.676</u>     | 0.415           | <u>0.621</u>     | <u>0.570</u>         | <u>0.715</u>     |
| East Bay  | 0.002           | 0.473            | 0.041           | 0.331            | 0.090           | 0.366            | 0.043                | 0.367            |
| Galveston Bay, South                                  | 0.426           | 0.468            | 0.426           | <u>0.511</u>     | 0.381           | 0.485            | 0.417                | 0.497            |
| Bay totals  | 0.445           | 0.415            | 0.413           | 0.496            | 0.376           | 0.484            | 0.412                | 0.477            |

<sup>a</sup>The time-weighted inflow condition is the time-weighted average of the three freshwater inflow scenarios calculated from equation 9. A value above 0.5 (underlined) indicates a net positive effect of the future hydrology. The bay areas are condensations of the 18 bay areas depicted in Figure 4: West Bay (West Bay, West; West Bay, Central), Trinity Bay (Trinity Bay, Southeast; Trinity Bay, Northwest), Galveston Bay, North (Clear Lake Embayment; Red Bluff to Morgan Point; Galveston Bay, North; Trinity Bay, Southwest; Houston Ship Channel, Clear Lake Reach; Houston Ship Channel, Morgan Point Reach), East Bay (East Bay, West; East Bay, East), Galveston Bay, South (Pelican Island Embayment; Texas City to Dollar Point; Dickinson Embayment; Galveston Bay, Central; Houston Ship Channel, Dickinson Embayment Reach; Houston Ship Channel, Texas City Reach).

positively and negatively affected by the change in environmental conditions. This approach minimizes the effect of selected areas, such as the Pelican Island Embayment, that are likely to be less accurately simulated than the majority, on the final evaluation. For each comparison, the total oyster abundance and the abundance of market-size ( $\geq 76$  mm) oysters is given. Differences between simulations are explained by examining the effect of a change in environmental conditions on oyster fecundity, larval survivorship, mortality from *Perkinsus marinus* infection, and mortality from reduced salinity.

#### 2024 Hydrology

By 2024, freshwater inflow into the Galveston Bay system is anticipated to be somewhat reduced relative

to 1993 (cf. Figures 2B and 3B), but more importantly, the amount of freshwater diverted from the Trinity River drainage basin to the Houston metropolitan area is anticipated to be substantially increased. Simulations show that market-size abundance declines in about two thirds of bay reef acreage under 2024 conditions in comparison to 1993. Declines are most pronounced under low freshwater inflow conditions in West and East Bay and under mean inflow conditions in West Bay and south Galveston Bay (Table 1, Figure 5A). The central and upper bay are, to a large extent, unimpacted and, under conditions of high freshwater inflow, improve significantly. In general, between 50% and 70% of the reef acreage is positively affected by the 2024 hydrology in most upper and central bay regions

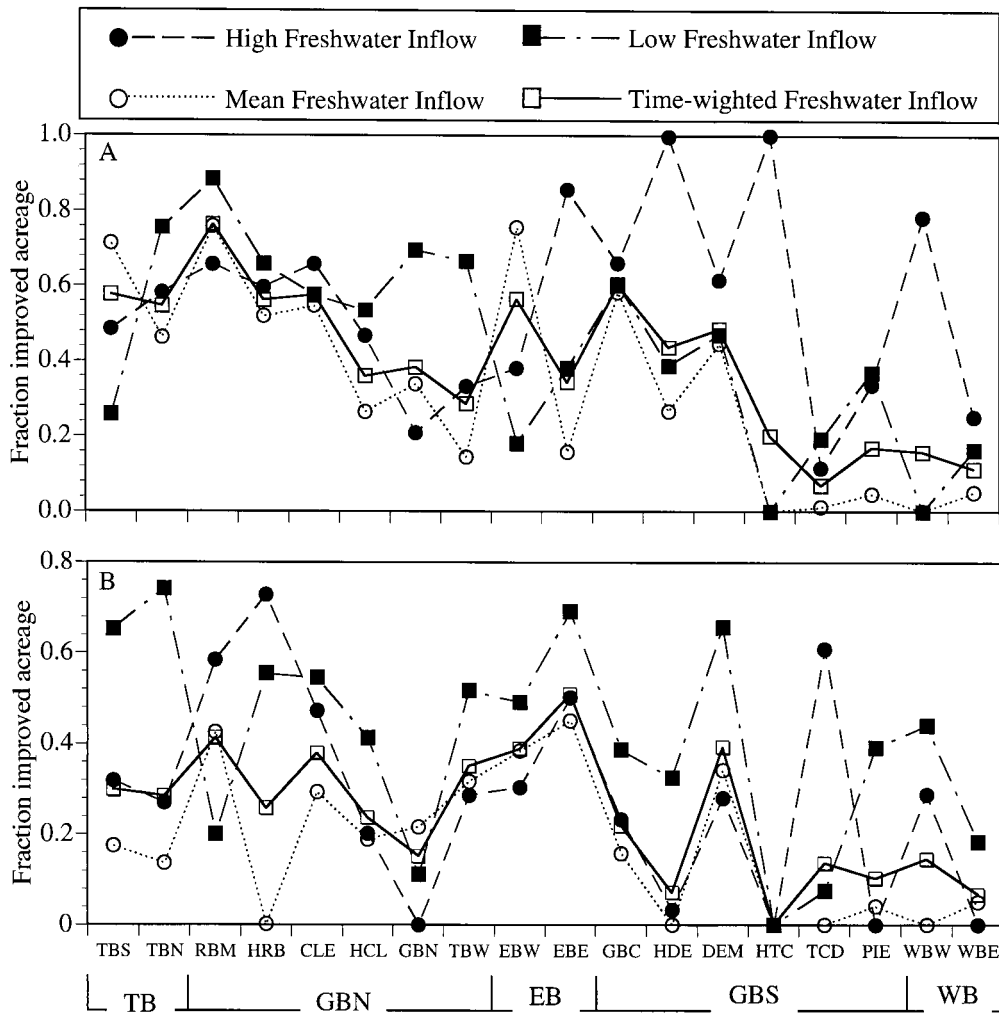


**Figure 5.** Results of simulations showing reef acreage positively impacted by the (A) 2024 and (B) 2049 hydrologies when compared to the 1993 hydrology for high, mean, and low freshwater inflows and for the time-weighted average of the three freshwater inflows. Positive impact is based on simulated changes in market-size oyster abundance. Abbreviations are: Trinity Bay (TB) [including Trinity Bay, Southeast (TBS); Trinity Bay, Northwest (TBN)], Galveston Bay, North (GBN) [including Red Bluff to Morgan Point (RBM); Houston Ship Channel, Morgan Point Reach (HRB); Clear Lake Embayment (CLE); Houston Ship Channel, Clear Lake Reach (HCL); Galveston Bay, North; Trinity Bay, Southwest (TBW)], East Bay (EB) [including East Bay, West (EBW); East Bay, East (EBE)], Galveston Bay, South (GBS) [including Galveston Bay, Central (GBC); Houston Ship Channel, Dickinson Embayment Reach (HDE); Dickinson Embayment (DEM); Houston Ship Channel, Texas City Reach (HTC); Texas City to Dollar Point (TCD); Pelican Island Embayment (PIE)], West Bay (WB) [including West Bay, West (WBW); West Bay, Central (WBE)].

(Figures 5A and 6A, Table 1). Total oyster abundance is more grievously impacted by the 2024 hydrology (Figure 6B, Table 1). Seventy-five percent of all reef acreage suffers a reduction in total oyster abundance. The West Bay and East Bay arms are again significantly affected; however, Galveston Bay proper is impacted, particularly west of the Houston Ship Channel up-bay of Redfish Bar and under mean freshwater inflow conditions.

The lesser effect of the 2024 hydrology on market-

size oysters in comparison to total oysters suggests that increased mortality from *P. marinus* is an unlikely explanation for the overall reduction in the oyster population. Simulations show that the 2024 hydrology increases the impact of *P. marinus* on oysters in Galveston Bay; however, the impact is not great and is limited primarily to the highest salinity regions of lower Galveston Bay proper and West Bay (Figure 7A, Table 2). Mortality from low salinity likewise rises somewhat,

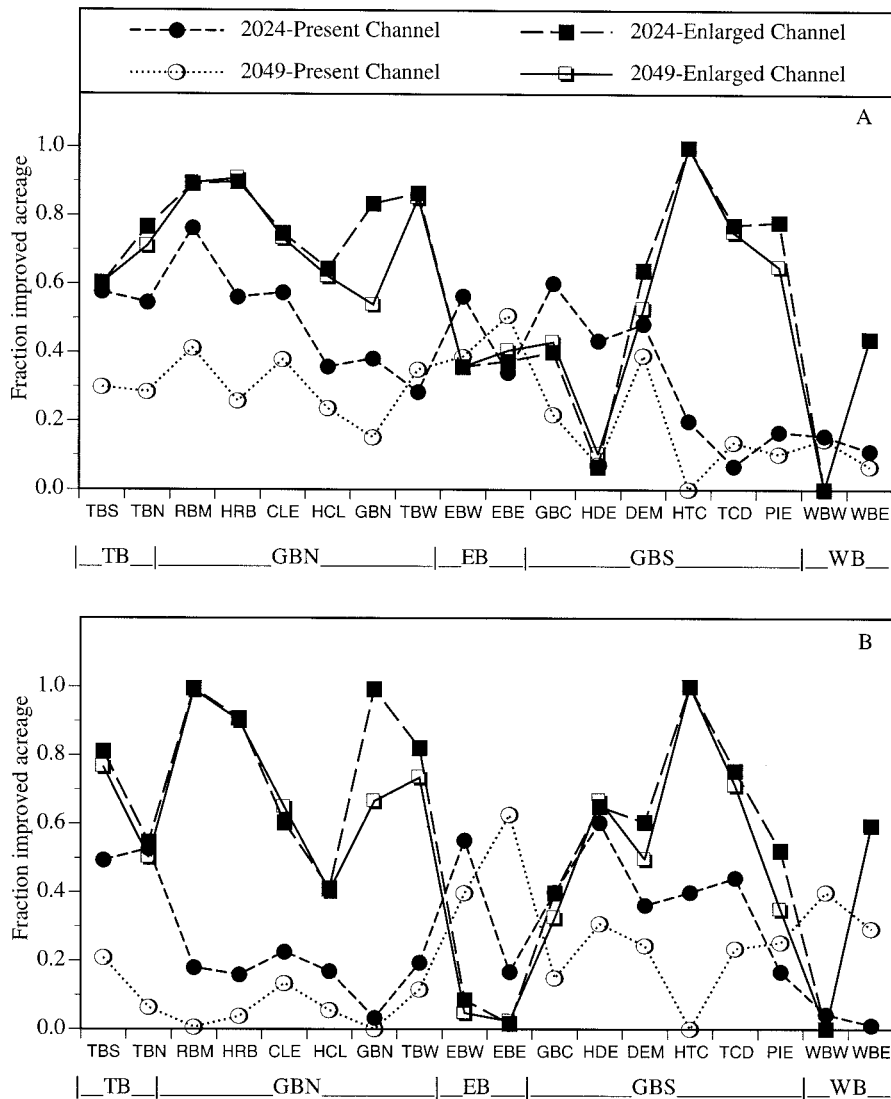


**Figure 6.** Results of simulations showing the fraction of reef acreage positively impacted by the 2024 or 2049 hydrologies when compared to the 1993 hydrology with the present or enlarged ship channel configuration for the time-weighted average of the three freshwater inflows. Positive impact is based on estimated changes in (A) market-size oyster abundance and (B) total oyster abundance. Abbreviations are given in Figure 5.

but is of limited importance. Fecundity declines, however, and these declines occur predominantly west of the Houston Ship Channel and in West Bay (Figure 7B, Table 3), and are particularly pronounced under mean freshwater inflow conditions. This pattern follows that observed for total oyster abundance (Figure 6B, Table 1). Larval survivorship does not decline to an equivalent extent overall (Figure 7C, Table 4), although declines are significant throughout Galveston Bay west of the Houston Ship Channel and in West Bay. Hence, the widespread reduction in total oyster abundance originates from a reduction in fecundity and larval survival

rather than a reduction in broodstock and is concentrated west of the Houston Ship Channel in the region receiving increased freshwater inflow from the diversion of Trinity River water.

#### 2049 Hydrology

By 2049, freshwater inflow is anticipated to increase substantially as greater amounts of freshwater are imported from drainage basins beyond the Galveston Bay watershed. Most of this freshwater will enter the drainage basins draining the Houston metropolitan area,

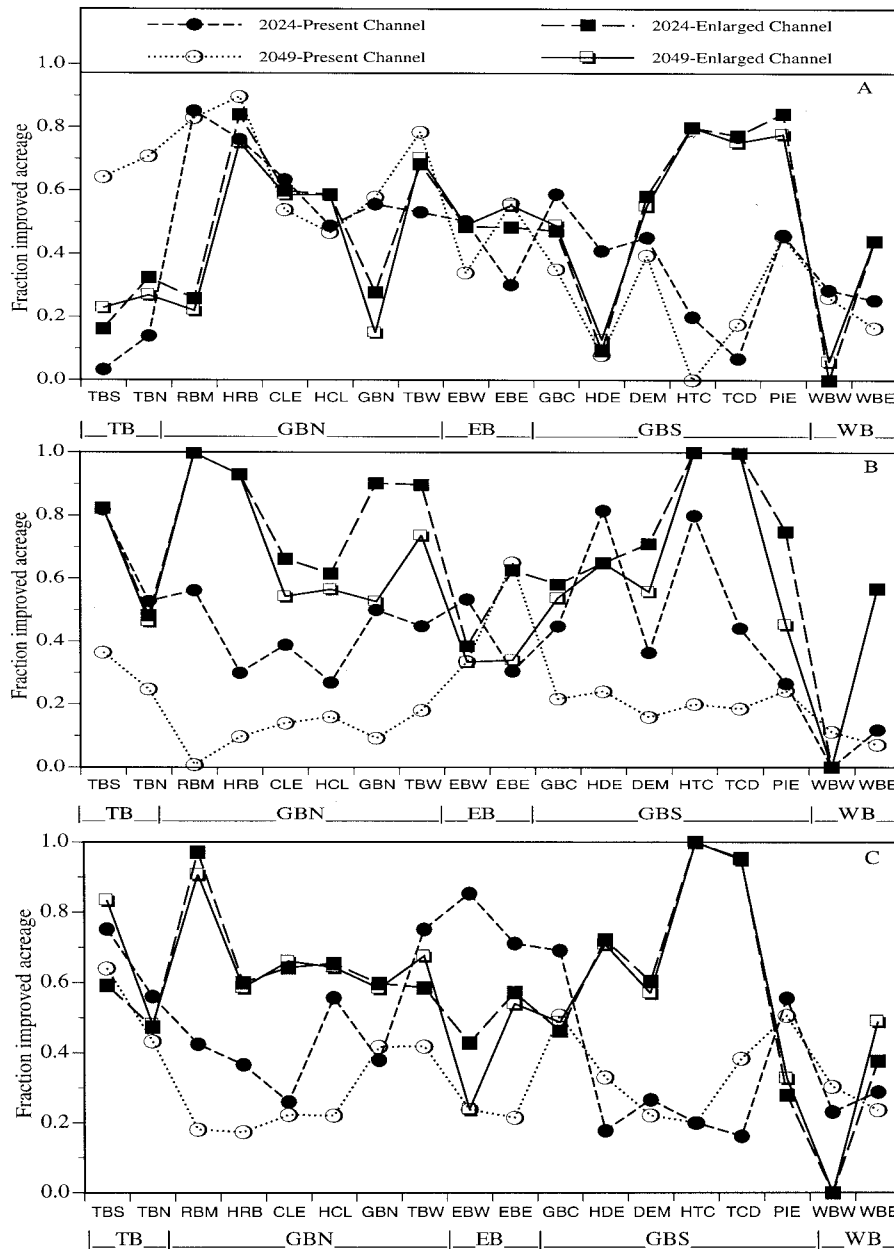


**Figure 7.** Results of simulations showing the fraction of reef acreage with (A) reduced mortality from *Perkinsus marinus* infection, (B) increased fecundity, and (C) increased larval survivorship under the 2024 or 2049 hydrology when compared to the 1993 hydrology with the present or enlarged ship channel configuration for the time-weighted average of the three freshwater inflows. Positive impact is based on estimated changes in the market-size population. Abbreviations are given in Figure 5.

principally the San Jacinto River and Buffalo Bayou, exacerbating the impact of diversion of Trinity River water to the Houston metropolitan area. A comparison of simulations of 1993 and 2049 conditions shows that market-size abundance declines over the vast majority of all bay reef acreage under 2049 conditions (Figure 5B). Declines exceeded those recorded for the 2024

hydrology in nearly all bay areas (Figure 6A). With few exceptions, declines are most pronounced under mean and high freshwater inflow conditions (Figure 5B, Table 1). Total oyster abundance also declined significantly (Figure 6B, Table 1). Declines exceeded those recorded for the 2024 hydrology in all bay areas except West Bay and the up-estuary end of East Bay (Figure

Table 2. Fraction of total bay acreage of oyster reef in Galveston Bay in which mortality from *Perkinsus marinus* infection declined as a proportion of the market-size population with the 2024 or 2049 hydrology compared to the 1993 hydrology under conditions of low, mean, and high freshwater inflow and the present or the enlarged ship channel configuration<sup>a</sup>

|   | High Inflow  | Mean Inflow  | Low Inflow   | Time-weighted Inflow |
|---|--------------|--------------|--------------|----------------------|
| 2024 vs 1993 hydrology, present channel configuration |              |              |              |                      |
| West Bay  | 0.358        | 0.272        | 0.129        | 0.260                |
| Trinity Bay   | 0.216        | 0.067        | 0.192        | 0.122                |
| Galveston Bay, North                                  | <u>0.687</u> | <u>0.712</u> | 0.350        | <u>0.634</u>         |
| East Bay  | <u>0.519</u> | <u>0.603</u> | 0.024        | 0.471                |
| Galveston Bay, South                                  | <u>0.503</u> | <u>0.515</u> | 0.357        | 0.481                |
| Bay totals  | 0.480        | 0.468        | 0.233        | 0.423                |
| 2049 vs 1993 hydrology, present channel configuration |              |              |              |                      |
| West Bay  | 0.059        | 0.254        | 0.109        | 0.186                |
| Trinity Bay   | <u>0.922</u> | <u>0.812</u> | 0.124        | <u>0.696</u>         |
| Galveston Bay, North                                  | 0.487        | <u>0.607</u> | <u>0.585</u> | <u>0.579</u>         |
| East Bay  | 0.469        | 0.418        | 0.157        | 0.376                |
| Galveston Bay, South                                  | 0.350        | 0.371        | 0.391        | 0.371                |
| Bay totals  | 0.322        | 0.397        | 0.293        | 0.361                |
| 2024 vs 1993 hydrology, enlarged ship channel         |              |              |              |                      |
| West Bay  | 0.000        | 0.440        | 0.440        | 0.352                |
| Trinity Bay   | 0.000        | 0.418        | 0.228        | 0.296                |
| Galveston Bay, North                                  | <u>0.711</u> | <u>0.512</u> | <u>0.720</u> | <u>0.594</u>         |
| East Bay  | <u>0.690</u> | 0.320        | <u>0.780</u> | 0.486                |
| Galveston Bay, South                                  | <u>0.517</u> | <u>0.622</u> | 0.499        | <u>0.576</u>         |
| Bay totals  | 0.395        | 0.498        | <u>0.546</u> | 0.487                |
| 2049 vs 1993 hydrology, enlarged ship channel         |              |              |              |                      |
| West Bay  | 0.059        | 0.440        | 0.440        | 0.364                |
| Trinity Bay   | 0.000        | 0.369        | 0.204        | 0.262                |
| Galveston Bay, North                                  | <u>0.733</u> | 0.487        | <u>0.722</u> | <u>0.583</u>         |
| East Bay  | <u>0.711</u> | 0.331        | <u>0.802</u> | <u>0.501</u>         |
| Galveston Bay, South                                  | <u>0.521</u> | <u>0.608</u> | 0.446        | <u>0.558</u>         |
| Bay totals  | 0.420        | 0.489        | <u>0.529</u> | 0.483                |

<sup>a</sup>The time-weighted inflow condition is the time-weighted average of the three freshwater inflow scenarios calculated from equation 9. A value above 0.5 (underlined) indicates a net positive effect of the future hydrology. The bay areas are condensations of the 18 bay areas depicted in Figure 4 as defined in Table 1.

6B). In the worst case, mean freshwater inflow conditions, just under 90% of all reef acreage suffers a reduction in total oyster abundance under 2049 conditions.

The 2049 hydrology exerts a significantly greater negative impact on Galveston Bay oyster populations than does the 2024 hydrology despite the increase in total freshwater inflow. The expanded area of decline in market-size oyster abundance under the 2049 hydrology in comparison to the 2024 hydrology suggests that increased adult mortality is partially responsible. Simulations show that the 2049 hydrology increases the impact of *P. marinus* on oysters in Galveston Bay over 2024 conditions, with most of this differential coming from greater mortality rates in central Galveston Bay along Hanna Reef, Redfish Bar, and into the Dickinson Embayment (Figure 7A, Table 2). Mortality from low salinity likewise rises, particularly under conditions of

high freshwater inflow, west of the Houston Ship Channel where most of the additional freshwater enters the bay from the Houston metropolitan area. Fecundity declines precipitously over most of Galveston Bay under 2049 conditions, falling well below even the depressed levels of 2024 (Figure 7B, Table 3). Declines are substantial in all bay regions. Larval survivorship does not decline to an equivalent extent, although larval survivorship falls consistently below 2024 conditions, with declines most noticeable in Galveston Bay north of Redfish Bar and into East Bay (Figure 7C, Table 4). Larval survivorship declines precipitously under mean freshwater inflow conditions throughout Galveston Bay, but is relatively unchanged from 2024 under conditions of low freshwater inflow. Hence, the widespread reduction in total oyster abundance in the 2049 simulation originates from a reduction in fecundity, increased adult mortality from *P. marinus* infection

Table 3. Fraction of total bay acreage of oyster reef in Galveston Bay in which fecundity increased as a result of the 2024 or 2049 hydrology compared to the 1993 hydrology under conditions of low, mean, and high freshwater inflow and the present or the enlarged ship channel configuration<sup>a</sup>

|   | High Inflow  | Mean Inflow  | Low Inflow   | Time-weighted Inflow |
|---|--------------|--------------|--------------|----------------------|
| 2024 vs 1993 hydrology, present channel configuration |              |              |              |                      |
| West Bay  | 0.427        | 0.014        | 0.000        | 0.094                |
| Trinity Bay   | 0.292        | <u>0.722</u> | 0.438        | <u>0.579</u>         |
| Galveston Bay, North                                  | 0.400        | 0.291        | <u>0.629</u> | 0.381                |
| East Bay  | 0.176        | <u>0.641</u> | 0.385        | 0.497                |
| Galveston Bay, South                                  | 0.449        | 0.336        | <u>0.555</u> | 0.402                |
| Bay totals  | 0.390        | 0.289        | 0.369        | 0.325                |
| 2049 vs 1993 hydrology, present channel configuration |              |              |              |                      |
| West Bay  | 0.000        | 0.014        | 0.355        | 0.080                |
| Trinity Bay   | 0.297        | 0.098        | <u>0.752</u> | 0.269                |
| Galveston Bay, North                                  | 0.083        | 0.009        | <u>0.550</u> | 0.132                |
| East Bay  | 0.065        | 0.498        | 0.380        | 0.388                |
| Galveston Bay, South                                  | 0.182        | 0.118        | <u>0.545</u> | 0.216                |
| Bay totals  | 0.099        | 0.121        | 0.473        | 0.187                |
| 2024 vs 1993 hydrology, enlarged ship channel         |              |              |              |                      |
| West Bay  | 0.453        | 0.453        | 0.453        | 0.453                |
| Trinity Bay   | <u>0.842</u> | 0.488        | <u>0.794</u> | <u>0.620</u>         |
| Galveston Bay, North                                  | <u>0.874</u> | <u>0.784</u> | 0.480        | <u>0.741</u>         |
| East Bay  | 0.133        | <u>0.541</u> | 0.369        | 0.425                |
| Galveston Bay, South                                  | <u>0.704</u> | <u>0.739</u> | 0.433        | <u>0.671</u>         |
| Bay totals  | <u>0.565</u> | <u>0.622</u> | 0.452        | <u>0.576</u>         |
| 2049 vs 1993 hydrology, enlarged ship channel         |              |              |              |                      |
| West Bay  | 0.453        | 0.453        | 0.453        | 0.453                |
| Trinity Bay   | <u>0.879</u> | 0.468        | <u>0.738</u> | <u>0.604</u>         |
| Galveston Bay, North                                  | <u>0.788</u> | <u>0.670</u> | 0.466        | <u>0.653</u>         |
| East Bay  | 0.101        | 0.402        | 0.369        | 0.335                |
| Galveston Bay, South                                  | <u>0.677</u> | <u>0.537</u> | 0.427        | <u>0.543</u>         |
| Bay totals  | <u>0.538</u> | <u>0.511</u> | 0.445        | <u>0.503</u>         |

<sup>a</sup>The time-weighted inflow condition is the time-weighted average of the three freshwater inflow scenarios calculated from equation 9. A value above 0.5 (underlined) indicates a net positive effect of the future hydrology. The bay areas are condensations of the 18 bay areas depicted in Figure 4 as defined in Table 1.

and, in the case of the higher impact noticeable under mean freshwater inflow conditions, a reduction in larval survival.

#### Enlarged Ship Channel—2024 Hydrology

Enlarging the Houston Ship Channel would result in increased salt intrusion into Galveston Bay. Because the impact of out-year hydrologies is negative and seems to be due mostly to a diversion of freshwater to drainage basins west of the Houston Ship Channel, the possibility exists that the enlarged channel would ameliorate the impact of these hydrologies.

Enlargement of the Houston Ship Channel negates the negative effect of the 2024 hydrology and, as a result, market-size abundance increases over much of Galveston Bay (Figure 6A). Baywide averages hover around 50% of reef acreage positively affected, however, because central Galveston Bay into East Bay, where most of the reef acreage is located, is not as

positively affected as other bay areas (Table 1). Precisely the same pattern is observed in total oyster abundance (Figure 6B, Table 1), except that total oyster abundance declines to very low levels in East Bay. Low freshwater inflow tends to minimize the positive effect of the enlarged ship channel, particularly in northern and southern Galveston Bay.

Mortality due to *P. marinus* infection is lower in lowermost Galveston Bay proper and higher in Trinity Bay than under present-day conditions (Table 2, Figure 7A). Overall, the impact of *P. marinus* is lessened with the larger ship channel, in 2024. The impact of mortality from exposure to low salinity also declines. Fecundity is improved throughout the bay system and is significantly higher in many bay regions relative to 1993 conditions with the enlarged ship channel than without it (Figure 7B, Table 3). Larval survivorship increased with the enlarged ship channel on reefs located west of the Houston Ship Channel and in northern Galveston Bay in 2024 in com-

Table 4. Fraction of total bay acreage of oyster reef in Galveston Bay in which larval survivorship increased as a result of the 2024 or 2049 hydrology compared to the 1993 hydrology under conditions of low, mean, and high freshwater inflow and the present or the enlarged ship channel configuration<sup>a</sup>

|   | High Inflow  | Mean Inflow  | Low Inflow   | Time-weighted Inflow |
|---|--------------|--------------|--------------|----------------------|
| 2024 vs 1993 hydrology, present channel configuration |              |              |              |                      |
| West Bay  | <u>0.881</u> | 0.126        | 0.123        | 0.276                |
| Trinity Bay   | <u>0.700</u> | 0.423        | <u>1.000</u> | <u>0.594</u>         |
| Galveston Bay, North                                  | 0.318        | 0.469        | <u>0.756</u> | 0.497                |
| East Bay  | <u>0.689</u> | <u>0.944</u> | <u>0.624</u> | <u>0.829</u>         |
| Galveston Bay, South                                  | 0.418        | <u>0.537</u> | <u>0.537</u> | <u>0.513</u>         |
| Bay totals  | <u>0.592</u> | 0.454        | 0.477        | 0.486                |
| 2049 vs 1993 hydrology, present channel configuration |              |              |              |                      |
| West Bay  | <u>0.782</u> | 0.000        | 0.465        | 0.249                |
| Trinity Bay   | <u>0.654</u> | 0.271        | <u>0.882</u> | 0.470                |
| Galveston Bay, North                                  | <u>0.689</u> | 0.154        | 0.406        | 0.311                |
| East Bay  | 0.332        | 0.001        | <u>0.838</u> | 0.235                |
| Galveston Bay, South                                  | <u>0.549</u> | 0.300        | <u>0.637</u> | 0.417                |
| Bay totals  | <u>0.616</u> | 0.142        | <u>0.585</u> | 0.325                |
| 2024 vs 1993 hydrology, enlarged ship channel         |              |              |              |                      |
| West Bay  | 0.453        | 0.282        | 0.201        | 0.300                |
| Trinity Bay   | <u>0.538</u> | 0.321        | <u>0.970</u> | 0.494                |
| Galveston Bay, North                                  | <u>0.710</u> | <u>0.549</u> | <u>0.679</u> | <u>0.607</u>         |
| East Bay  | <u>0.549</u> | 0.425        | 0.433        | 0.451                |
| Galveston Bay, South                                  | 0.388        | 0.496        | <u>0.575</u> | 0.490                |
| Bay totals  | 0.488        | 0.422        | 0.473        | 0.446                |
| 2049 vs 1993 hydrology, enlarged ship channel         |              |              |              |                      |
| West Bay  | 0.389        | 0.453        | 0.201        | 0.390                |
| Trinity Bay   | <u>0.561</u> | 0.389        | <u>0.981</u> | <u>0.542</u>         |
| Galveston Bay, North                                  | <u>0.676</u> | <u>0.599</u> | <u>0.684</u> | <u>0.632</u>         |
| East Bay  | <u>0.561</u> | 0.154        | 0.422        | 0.289                |
| Galveston Bay, South                                  | 0.385        | <u>0.503</u> | <u>0.594</u> | 0.497                |
| Bay totals  | 0.465        | 0.450        | 0.480        | 0.459                |

<sup>a</sup>The time-weighted inflow condition is the time-weighted average of the three freshwater inflow scenarios calculated from equation 9. A value above 0.5 indicates a net positive effect of the future hydrology. The bay areas are condensations of the 18 bay areas depicted in Figure 4 as defined in Table 1.

parison to the same hydrology with the present channel configuration (Figure 7C, Table 4). However, larval survivorship was lower across Redfish Bar and into East Bay with the enlarged ship channel in the same comparison and the amount of reef in these latter two areas was sufficient to limit the positive effect of channel enlargement overall (Table 4).

#### Enlarged Ship Channel—2049 Hydrology

Enlargement of the Houston Ship Channel negates the negative effect of the 2049 hydrology, just as it did for the 2024 hydrology, by allowing market-size oyster abundance to increase over much of Galveston Bay (Figure 6A). Baywide averages hover around 50% of reef acreage positively affected, however, because Redfish Bar into East Bay, where most of the reef acreage is located, is not as positively affected as other bay areas (Figure 6A, Table 1), as was also seen in the 2024 comparison. Precisely the same pattern is observed in total oyster abundance (Figure 6B, Table 1).

Mortality due to *P. marinus* infection is lower in lowermost Galveston Bay proper and higher in Trinity Bay than under present-day conditions (Table 2, Figure 7A). Overall, the impact of *P. marinus* is lessened with the larger ship channel in the 2049 simulation, as seen in the 2024 simulation. The impact of mortality from exposure to low salinity also follows the pattern observed in the 2024 comparison. As in the 2024 comparison, fecundity is improved throughout the bay system and is significantly higher relative to 1993 conditions with the enlarged ship channel than without it (Figure 7B, Table 3). Larval survivorship increased with the enlarged ship channel on reefs located west of the Houston Ship Channel and in Trinity Bay in 2049 in comparison to the same hydrology with the present channel configuration, as it did in the 2024 comparison (Figure 7C, Table 4). Thus, the influence of channel enlargement in 2049 was nearly identical to the influence of channel enlargement in 2024, in that much of the negative impact of the anticipated changes in fresh-

water inflow are negated by channel enlargement and the subsequent increased transport of salt upbay.

## Discussion

### Impact of Hydrology

With the exception of East Bay, the 2024 and 2049 hydrologies result in declines in abundance over the majority of reef acreage, but only for total oyster abundance (Figure 6B). Typically more than 50% and often more than 70% of the reef acreage in Galveston Bay is negatively impacted by these hydrologies. Typically, reefs west of the Houston Ship Channel from Eagle Point to Morgan Point, reefs along the Houston Ship Channel, and reefs south of Smith Point show greater than average declines. Similar changes occur on oyster reefs in West Bay. Reefs in East Bay and in parts of Trinity Bay show greater than average increases. The 2049 pattern was reasonably similar; however, less acreage was positively affected.

Market-size abundance is somewhat less impacted than total abundance (Figure 6). However, this result is partially due to the short simulation time of only two years that is well within the lifespan of a single oyster generation. One would anticipate that the results for market-size oyster abundance would come into conformity with the results for total oyster abundance over time and, thus, the negative impacts estimated from total oyster abundance more likely approximate the long-term condition.

Low freshwater inflow produced a more widespread gain in abundance in the central bay in 2024 and 2049 than mean freshwater inflow, and this was particularly obvious in 2049, although, overall, abundances still declined (Figure 5). Thus, low freshwater inflow tended to minimize the negative impact of both hydrologies.

In the simulations, adult mortality is principally produced by *P. marinus* infection. A variety of factors, including fecundity and larval survivorship, affect total oyster abundance by controlling recruitment. In addition, some mortality factors such as exposure to low salinity, do not discriminate across size classes. The hydrologies have only a limited effect on *P. marinus*-produced mortality, in keeping with the more limited impact of the hydrologies on the market-size population. Fecundity is lower, particularly in 2049, and larval survivorship is lower in both the 2024 and 2049 hydrologies. Thus, the negative impact of the two hydrologies originates in factors limiting recruitment, in large measure.

The larger negative impact in 2049 originates from

the larger drop in fecundity under that hydrology. Differences in fecundity between simulations are modulated principally by changes in *P. marinus* infection intensity, not mortality, and salinity. Salinities below 15‰ impose an additional energy demand on the adults, which can result in a reduction in fecundity (Hofmann and others 1992, Barber 1996). Higher *P. marinus* infection intensities also impose an energy demand on the adults that can reduce fecundity (Cox and Mann 1992, Hofmann and others 1995, Barber 1996). *P. marinus* infection intensities do rise under both hydrologies. The decline in total freshwater inflow from the Trinity River promotes the development of *Perkinsus marinus* epizootics in the reefs most down-estuary in southern Galveston Bay and in East Bay (Figure 7A).

In the simulations, increased larval mortality is primarily produced by lower salinity. Larval survivorship declines throughout much of the bay system except East Bay (Figure 7C). Low salinity can result in direct larval mortality, but the primary effect of low salinity is to increase larval planktonic time, thereby exposing the larvae to planktonic predators for longer periods. As a consequence, survivorship declines.

These simulation comparisons illustrate the deleterious effects that can result from a reduction in freshwater inflow into Trinity Bay and an increase in freshwater inflow west of the Houston Ship Channel that is the anticipated effect of freshwater diversion from the Trinity River watershed to serve the needs of the Houston metropolitan area. The primary result of the diversion of freshwater from the Trinity River to the San Jacinto River is to vary the salinity structure such that the bay west of the Houston Ship Channel remains fresher during the spring and early summer while salinity rises south of Eagle Point and Smith Point. The bay area west of the Houston Ship Channel from Eagle Point to Morgan Point represents a much smaller volume than does Trinity Bay. This smaller volume is less able to buffer increased freshwater inflows so that salinity drops on the western side of the bay more quickly and to a greater extent during periods of high freshwater inflow. Thus, much of the negative impact north of a line from Eagle Point to Smith Point is produced by an increase in mortality of larvae and adults and a reduction in scope for growth and, consequently, fecundity imposed by the influence of freshwater coming down the San Jacinto River and Buffalo Bayou. The lesser impact of the hydrologies under conditions of low freshwater inflow occurs because low freshwater inflow minimizes the influence of water diversion by increasing salt transport up the western side of the bay.

### Ship Channel Enlargement

Oyster abundance and biomass are predicted to increase with ship channel enlargement (Klinck and others, 2002). The amount of bay acreage positively affected by channel enlargement averages about 53%. Declines were noted in most simulations in West Bay, East Bay, on part of Redfish Bar, and along the lower-most reaches of the Houston Ship Channel. These declines were more than balanced by increased abundance and biomass elsewhere. As the enlarged channel increases saltwater intrusion, the results of Klinck and others (2002) seem, at first, to be counterintuitive because rising salinity is usually deleterious to oyster populations. The solution to the conundrum posed by increased oyster production with increased saltwater intrusion can be found in the interaction of historical changes in bay physiography with the changes in freshwater inflow anticipated in the first half of the 21st century.

The 20th century history of Galveston Bay is one of expansion of the salinity gradient and increased oyster production. Prior to 1940, the salinity gradient of the bay was compressed about Redfish Bar that acted as a dam to water flow in the bay. At that time, Redfish Bar extended from Eagle Point to Smith Point along the Chambers County Line (Powell and others 1995a) (Figure 1). Commercial production was limited to the western, down-estuary portion of the bay south of the single largest channel through this bar (located just behind what is presently called Redfish Island). (Redfish Island succumbed to wave erosion in the late 1990s and no longer exists as a supratidal entity.) Removal of this barrier reef dam and the addition of the present ship channel dramatically expanded the salinity gradient of the bay and permitted expansion of a commercial fishery in the early 1950s. Much of this fishery is located downestuary of the original Redfish Bar in an area that was specifically described in 1931 as unproductive (Galtsoff 1931). Thus, the present productivity of Galveston Bay is a result of anthropogenic intervention that has modified the hydrodynamic regime of Galveston Bay to sustain a greatly expanded salinity gradient in the bay. At present, much of the central reefal area, where the original barrier reefs were located, is just up-estuary of optimal conditions for oyster production. A disequilibrium exists between substrate availability and salinity structure. As a result, reefs have been expanding down-estuary from this region for the last 20 years in response to the mismatch between the best growing conditions as determined by salinity and food supply and the present location of hard substrate (Powell and others 1995a). Reefs have also been ac-

Table 5. Fraction of total acreage of oyster reef in Galveston Bay in which total and market-size ( $\geq 76$  mm) oyster biomass increased with the proposed larger channel configuration compared to the present configuration under the present, 2024, and 2049 hydrologies<sup>a</sup>

| Location                                  | Biomass |        |
|---|---------|--------|
|   | Total   | Market |
| West Bay, West                            | 0.000   | 0.014  |
| West Bay, Central                         | 0.568   | 0.479  |
| Pelican Island Embayment                  | 0.766   | 0.835  |
| Texas City to Dollar Point                | 0.824   | 0.848  |
| East Bay, West                            | 0.143   | 0.355  |
| East Bay, East                            | 0.140   | 0.447  |
| Galveston Bay, Central                    | 0.454   | 0.447  |
| Trinity Bay, Southeast                    | 0.923   | 0.696  |
| Trinity Bay, Northwest                    | 0.850   | 0.822  |
| Red Bluff to Morgan Point                 | 0.997   | 0.924  |
| Clear Lake Embayment                      | 0.732   | 0.758  |
| Dickinson Embayment                       | 0.732   | 0.663  |
| Galveston Bay, North                      | 0.929   | 0.849  |
| Trinity Bay, Southwest                    | 0.832   | 0.900  |
| Houston Ship Channel, Morgan Point Reach  | 0.887   | 0.902  |
| Houston Ship Channel, Clear Lake Reach    | 0.620   | 0.708  |
| Houston Ship Channel, Dickinson Em. Reach | 0.609   | 0.135  |
| Houston Ship Channel, Texas City Reach    | 1.000   | 1.000  |
| Bay totals                                | 0.527   | 0.532  |

<sup>a</sup>The fractions are a weighted averages (equations 9 and 10) of the three freshwater inflow scenarios (low, mean, high) and the three hydrologies (1993, 2024, 2049). Bay locations are defined in Figure 4.

tively expanding along and west of the Houston Ship Channel where the reefs are protected from the enhanced Trinity River flow around Smith Point that was likely produced by the removal of the barrier reefs that once bisected the bay between Eagle Point and Smith Point.

In principle, the additional saltwater influx produced by channel enlargement could ameliorate the negative impact of freshwater diversion in much the same way as the original channel permitted production to expand. The simulations support this intuitive expectation. The impact of the combination of anticipated hydrology and channel enlargement improves bay oyster production over present-day (1993) conditions in 70%–100% of many bay reaches (Table 5). Only East Bay, the southern edge of Redfish Bar, and middle West Bay are negatively impacted (Table 5). Those negative

impacts still remaining after the combination of channel enlargement and hydrological modifications are almost entirely due to increased *P. marinus* mortality, although the East and West Bay declines are exacerbated by a reduction in larval survivorship. East Bay, the southern edge of Redfish Bar, and middle West Bay are negatively impacted under both future hydrologies, 2024 and 2049, and also simply by channel enlargement. In the lower bay, increased salinity increases the susceptibility of oyster populations to *P. marinus* epizootics. Adult mortality rises, fecundities fall, and recruitment declines. Much of the affected area in West Bay is already unproductive as a result of *P. marinus* and higher predation rates. Channel enlargement and the changes in hydrology can be expected to also permanently reduce production on Hanna Reef, along the southern extent of South Redfish Reef, and from South Redfish Reef to Pasadena Reef. These latter two areas are sites of active reef accretion today as the reefs expand down-estuary in response to the bay's present salinity gradient and hydrodynamic structure.

Increased production elsewhere in the bay is due principally to the increase in salinity brought about by channel enlargement that improves growing conditions by removing the negative effects of low salinity on fecundity and larval survival. Improvement in these regions is only to a limited extent due to relaxation of the negative influence of *P. marinus* infection, although the rate of mortality declines and, very likely, the chance of epizootics is much reduced. The predicted damage produced by the anticipated future hydrologies is minimized by the enlarged ship channel because the down-estuary movement of the moderate salinities conducive to oyster growth produced by freshwater diversion is negated by an up-estuary movement of salt produced by channel enlargement. Freshwater diversion into the San Jacinto and Buffalo Bayou drainage basins places freshwater into the western side of the bay too close to actively growing reefs for saltwater mixing to limit the decline in salinity. The enlarged channel returns more optimal conditions to these reefs by the up-estuary movement of salt and by the lateral expansion of the salinity gradient subparallel to the Houston Ship Channel.

## Conclusions

Freshwater diversion to supply the Houston metropolitan area is predicted to negatively impact oyster production in Galveston Bay, because the mixing pool for the San Jacinto and Buffalo Bayou drainage basins is small in comparison to Trinity Bay and, as a consequence, salinity drops more quickly and to a greater

extent during periods of increased freshwater inflow. This negative effect is not balanced by the up-estuary movement of salt on the Trinity River side of the bay because little reef acreage exists in that area. As a result, even though total freshwater inflow into the bay is reduced only somewhat in 2024 and is actually increased in 2049, oyster production declines due to the disequilibrium that is produced between substrate availability and the new salinity structure imposed by freshwater diversion. Although the bay hydrology shifts, available hard substrate does not. By chance, the planned enlargement of the Houston Ship Channel would negate these negative effects and, in fact, increase production in substantial areas of the bay by reorienting the salinity gradient more favorably over the present hard substrate.

The vast bulk of reef expansion is occurring today within a restricted region around the Houston Ship Channel. Reefs are growing down-estuary and up-bay along the parallel-trending spoil banks in response to long-term changes in salinity structure. Further reef expansion can be anticipated on and north of Redfish Bar, from Buoy 63 on the ship channel north along the Houston Ship Channel, and, very likely, north and south of Red Bluff and in Trinity Bay following channel enlargement, assuming the anticipated future hydrologies also come to pass. What is crucial to this scenario, however, is channel enlargement. The diversion of freshwater alone significantly impacts oyster production and can be expected to greatly reduce the commercial industry should it alone come to pass. The simulations stress the point that it is not just the well-appreciated reduction in freshwater inflow that can cause negative impacts on oyster populations. Changing the location of freshwater inflow can also significantly impact the bay environment, even if the total amount of freshwater inflow remains unchanged.

What is not included in our model is the ability of oysters to expand hard substrate dramatically over a relatively short time frame. In Galveston Bay, minimally 2000 ha of new reef has been formed over a 20-yr period (Powell and others 1995a). Thus, the 2049 simulation and to some extent the 2024 simulation must be considered in the context of the ability of the oyster populations to substantially modify their habitat in a relatively short period of time. A more detailed evaluation of impact should take into account the likelihood of new oyster reef being produced on a large scale.

## Acknowledgments

This research was supported by a grant from the Army Corps of Engineers, Galveston District Office

DACW64-91-C-0040 to Texas A&M University and Old Dominion University. Additional computer resources and facilities were provided by the Center for Coastal Physical Oceanography at Old Dominion University.

### Literature Cited

- Andrews, J. D., and S. M. Ray. 1988. Management strategies to control the disease caused by *Perkinsus marinus*. *American Fisheries Society Special Publication* 18:257–264.
- Armstrong, N. E. 1982. Responses of Texas estuaries to freshwater inflows. Pages 103–120 in V. S. Kennedy (ed.), Proceedings of the 6th biennial international estuarine research conference. Academic Press, New York.
- Barber, B. J. 1996. Gametogenesis of eastern oysters, *Crassostrea virginica* (Gmelin, 1791), and Pacific oysters, *Crassostrea gigas* (Thunberg, 1793) in disease-endemic lower Chesapeake Bay. *Journal of Shellfish Research* 15:285–290.
- Berger, R. C., R. T. McAdory, J. H. Schmidt, and W. D. Martin. 1995. Houston-Galveston navigational channels, Texas project; Three-dimensional numerical modeling of hydrodynamics and salinity. United States Army Corps of Engineers, Waterways Experiment Station, Rpt. HL-92-7. Vicksburg, Mississippi.
- Butler, P. A. 1949. Gametogenesis in the oyster under conditions of depressed salinity. *Biological Bulletin (Woods Hole)* 96:263–269.
- Cox, C., and R. Mann. 1992. Temporal and spatial changes in fecundity of Eastern oysters, *Crassostrea virginica* (Gmelin, 1791) in the James River, Virginia. *Journal of Shellfish Research* 11:49–54.
- Davis, H. C. 1958. Survival and growth of clam and oyster larvae at different salinities. *Biological Bulletin (Woods Hole)* 114:296–307.
- Davis, H. C. 1964. Combined effects of temperature and salinity on development of eggs and growth of larvae of *M. mercenaria* and *C. virginica*. *United States Fish and Wildlife Service Fisheries Bulletin* 63:643–655.
- Deksheniaks, M. M., E. E. Hofmann, and E. N. Powell. 1993. Environmental effects on the growth and development of Eastern oyster, *Crassostrea virginica* (Gmelin, 1791), larvae: a modeling study. *Journal of Shellfish Research* 12:241–254.
- Deksheniaks, M. M., E. E. Hofmann, J. M. Klinck, and E. N. Powell. 1996. Modeling the vertical distribution of oyster larvae in response to environmental conditions. *Marine Ecology Progress Series* 136:97–110.
- Deksheniaks, M. M., E. E. Hofmann, J. M. Klinck, and E. N. Powell. 1997. A modeling study of the effects of size- and depth-dependent predation on larval survival. *Journal of Plankton Research* 19:1583–1598.
- Deksheniaks, M. M., E. E. Hofmann, J. M. Klinck, and E. N. Powell. 2000. Quantifying the effects of environmental change on an oyster population: a modeling study. *Estuaries* 23:593–610.
- Engle, J. B., and C. R. Chapman. 1953. Oyster condition affected by attached mussels. National Shellfisheries Association convention addresses for 1951, pp. 70–78.
- Fisher, W. L., J. H. McGowen, L. F. Brown, Jr., and C. G. Groat. 1972. Environmental geologic atlas of the Texas coastal zone Galveston-Houston area. Bureau of Economic Geology, Austin, Texas.
- Galtsoff, P. S. 1931. Survey of oyster bottoms in Texas. United States Bureau of Fisheries Investigations Rpt. 6, pp 1–30.
- Hidu, H., and H. H. Haskin. 1978. Swimming speeds of oyster larvae *Crassostrea virginica* in different salinities and temperatures. *Estuaries* 1:252–255.
- Hill, A. E. 1991. Vertical migration in tidal currents. *Marine Ecology Progress Series* 75:39–54.
- Hofmann, E. E., E. N. Powell, J. M. Klinck, and E. A. Wilson. 1992. Modeling oyster populations. III. Critical feeding periods, growth and reproduction. *Journal of Shellfish Research* 11:399–416.
- Hofmann, E. E., E. N. Powell, J. M. Klinck, and G. Saunders. 1995. Modeling diseased oyster populations I. Modelling *Perkinsus marinus* infections in oysters. *Journal of Shellfish Research* 14:121–151.
- Hofstetter, R. P. (revised by C. E. Bryan). 1990. The Texas oyster fishery. Bulletin No. 40. Texas Parks and Wildlife Department, Austin, Texas, 21 pp.
- Klinck, J. M., E. E. Hofmann, E. N. Powell, and M. M. Deksheniaks. 2002. Impact of channelization on oyster production: a hydrodynamic-oyster population model for Galveston Bay, Texas. *Environmental Modeling & Assessment* (in press).
- Loosanoff, V. L. 1953. Behavior of oysters in water of low salinities. *Proceedings of the National Shellfisheries Association* 43:135–151.
- McAdory, R. T., R. C. Berger, and W. D. Martin. 1995. Three-dimensional model and salinity results for use in an oyster model of Galveston Bay. Pages 27–36 in R. Jensen (ed.), Water for Texas. Proceedings of the 24th Water for Texas Conference.
- Moore, H. F. 1907. Survey of oyster bottoms in Matagorda Bay, Texas. United States Bureau of Fisheries Doc. 610, pp. 1–86.
- NCDC. 1985. National Climatic Data Center, U.S.A.F. Environmental Technical Application Center, Federal Building, Asheville, North Carolina.
- Powell, E. N. and R. J. Stanton, Jr. 1985. Estimating biomass and energy flow of molluscs in paleo-communities. *Palaeontology (London)* 28:1–34.
- Powell, E. N., E. E. Hofmann, J. M. Klinck, and S. M. Ray. 1992. Modeling oyster populations I. A commentary on filtration rate. Is faster always better? *Journal of Shellfish Research* 11:387–398.
- Powell, E. N., J. M. Klinck, E. E. Hofmann, M. M. Deksheniaks, E. A. Wilson-Ormond, and M. S. Ellis. 1995b. Galveston Bay Houston Ship Channel project, calculation of project impact, oyster population dynamics model. United States Army Corps of Engineers, Galveston District, Galveston, Texas.
- Powell, E. N., J. Song, M. S. Ellis, and E. A. Wilson-Ormond. 1995a. The status and long-term trends of oyster reefs in Galveston Bay, Texas. *Journal of Shellfish Research* 14:439–457.
- Powell, E. N., J. M. Klinck, E. E. Hofmann, and S. Ford. 1997.

- Varying the timing of oyster transplant: implications for management from simulation studies. *Fisheries Oceanography* 6:213–237.
- Quast, W. D., M. A. Johns, D. E. Pitts, Jr., G. C. Matlock, and J. E. Clark. 1988. Texas oyster fishery management plan. Fisheries Management Plan Series Number 1. Texas Parks and Wildlife Department, Coastal Fisheries Branch, Austin, Texas, 228 pp.
- Seliger, H. H., J. A. Boggs, R. B. Rivkin, W. H. Biggley, and K. R. H. Aspden. 1982. The transport of oyster larvae in an estuary. *Marine Biology (Berlin)* 71:57–72.
- Shumway, S. E. 1982. Oxygen consumption in oysters: an overview. *Marine Biology Letters* 3:1–23.
- Song, J. 1994. Spatial trends in commercially and health-related characteristics of Galveston Bay oyster reefs, Masters thesis. Texas A&M University, 113 pp.
- Soniat, T. M., and M. S. Brody. 1988. Field validation of a habitat suitability index model for the American oyster. *Estuaries* 11:87–95.
- Soniat, T. M., E. N. Powell, E. E. Hofmann, and J. M. Klinck. 1998. Understanding the success and failure of oyster populations: the importance of sampled variables and sample timing. *Journal of Shellfish Research* 17:1149–1165.
- Soniat, T. M., and J. D. Gauthier. 1989. The prevalence and intensity of *Perkinsus marinus* from the mid northern Gulf of Mexico, with comments on the relationship of the oyster parasite to temperature and salinity. *Tulane Studies in Zoology and Botany* 27:21–27.
- Ward Jr., G. H. 1980. Hydrography and circulation processes of Gulf estuaries. Pages 183–215 in P. Hamilton and K. B. MacDonald (eds.), *Estuarine and wetland processes with emphasis on modeling*. Plenum Press, New York.
- Wilson-Ormond, E. A., E. N. Powell, and S. M. Ray. 1997. Short-term and small-scale variation in food availability to natural oyster populations: food, flow and flux. *Pubblicazioni della Stazione Zoologica di Napoli I: Marine Ecology* 18:1–34.
- US ACE. 1995a. Engineering supplement to limited reevaluation report, Vol. 1. US Army Corps of Engineers Galveston District, Galveston, Texas.
- US ACE. 1995b. Houston-Galveston navigation channels, Texas limited reevaluation report and final supplemental environmental impact statement appendices. US Army Corps of Engineers, Galveston District, Galveston, Texas.